Journal of System Design and Dynamics

Vol. 3, No. 1, 2009

Skill Analysis of the Wrist Release in the Golf Swings Utilizing Shaft Elasticity*

Soichiro SUZUKI**, Yohei HOSHINO*** and Yukinori KOBAYASHI***

**Department of Mechanical System Engineering, Kitami Institute of Technology,
165 Koen-cho, Kitami, Hokkaido,090-8507 Japan
E-mail: zuki@mail.kitami-it.ac.jp

***Graduate school of Engineering, Hokkaido University,
N13W8, Sapporo, Hokkaido, 060-8628, Japan

Abstract

This study analyzes the skill component of the wrist release in the golf swing by employing a three-dimensional dynamic model considering vibration of the club shaft. It is observed that professional and expert golfers relax their wrists in the swing motion as a "natural" or "late" release. Thus, the relationship between the timing of the wrist release and the shaft vibration is examined in this study. First, it is demonstrated that "natural release" at the zero-crossing point of the bending vibration of the shaft efficiently increases the head speed at impact. In the next step, the "late hitting" condition is imposed upon the model. It is demonstrated that "late hitting" could further improve the efficiency of the swing motion. Finally, the skill component in the wrist release for the long drive is experimentally verified by measuring the movement of the wrist and the dynamic deformation of the shaft during the downswing.

Key words: Skill Analysis, Golf Swing, Late Hitting, Shaft Vibration, Zero-Crossing Point

1. Introduction

Previous studies analyzing golf swings have focused on improving the performance of golfers and golf clubs. Double pendulum models have been employed for computational investigations of golf swing, as a double pendulum is a physical model that expresses the movement of the shoulder and wrist with a rigid arm and the golf club. The early work of Cochlan and Stobbs[1] explained the ideal golf swing using a double pendulum model composed of two coplanar segments. In the kinetic and kinematic analyses of the double pendulum model, the relationship between the joint torque and the club motion is examined using inverse dynamics based upon image processing of the swing motion. Lampsa[2] investigated the joint torque that maximizes the head speed at impact. Budney and Bellow[3] demonstrated the effect of different types of clubs on the kinetics of the swing. Experimental results for the dynamics of the golf shaft, such as the results measured by Butler and Winfield[4], show that the shaft deformation caused by bending vibration during the downswing exceeds 6 inches, and it may therefore be expected that the shaft deformation strongly affects the swing motion.

Recent studies have examined the effect of shaft deformation on the trajectory of the launched ball. The analysis by Brylawski[5] showed that torsional deflection changes the face direction of the clubhead, and this torsional deflection affects the direction and the spin of the ball. Milne and Davis[6] have asserted that the bending flexibility of the shaft plays only a minor dynamic role, involving "whipping" in the pre-impact area. However, since the

*Received 24 Apr., 2008 (No. 08-0323)
[DOI: 10.1299/jsdd.3.47]

effect of the shaft deformation on a golfer's motion has not been examined, the actual effect on the ball cannot be computed.

This study analyzes the wrist release in the downswing using a three-dimensional dynamic model based on the double pendulum and includes the effects of forearm supination and three-dimensional shaft vibration. It is generally known that professional and expert golfers try to match shaft flexibility with their swing style, which is characterized by "natural" or "late" release. Jorgensen [7] obtained numerical solutions for the effect of a delayed wrist release. Vaughan [8] and Neal and Wilson [9] examined the wrist release in the downswing using a summation of three-dimensional forces and torques applied to the club. Pickering and Vickers [10] numerically showed the effect of "natural release" and "late hit" by a two-dimensional rigid double pendulum model. These results suggest that delaying the wrist release enhances the clubhead speed at impact.

Different from these reports, the results of the simulation performed by Springs and Mackenzie [11] have indicated that there is only a small advantage in employing the delayed release technique. The two-dimensional model in the Springs and Mackenzie simulation consists of three segments that consider the rotation of the shoulder around the spine. However, the model employed an unrealistic resistive torque of the wrist to delay the wrist release. The objective of this study is to demonstrate the effect of a natural delayed release of the wrist in conjunction with utilizing shaft elasticity, which has not so far been reported. Thus, it is expected that the results of this study will contribute to improving the performance of golfers and golf clubs by examining the relationship between the timing of the wrist release and shaft vibrations. First, it is demonstrated that a "natural release" with no acceleration torque at the zero-crossing point for the bending vibration of the club shaft can efficiently increase the head speed at impact. In the next step, the "late hitting" condition is imposed upon the model by using the examined acceleration of the shoulder. It is also demonstrated that "late hitting" can further improve the efficiency of the swing motion. Finally, the skill of the wrist release for a long drive is experimentally verified by measuring the movement of the wrist and the dynamic deformation of the shaft for various golfer ability levels.

2. Modeling

2.1 Simplified dynamic model

In the golf swing analysis, a three-dimensional dynamic model is simplified as shown in Fig. 1(a). The model defines an absolute coordinate system O-$X_1Y_1Z_1$ and a rotational coordinate system o'-xyz, which is fixed at the grip side of the shaft. The rotational angles of the shoulder and wrist from the X_1 axis are expressed by θ_1 and θ_2, respectively. The downswing is assumed to be performed in a plane so that the double pendulum model

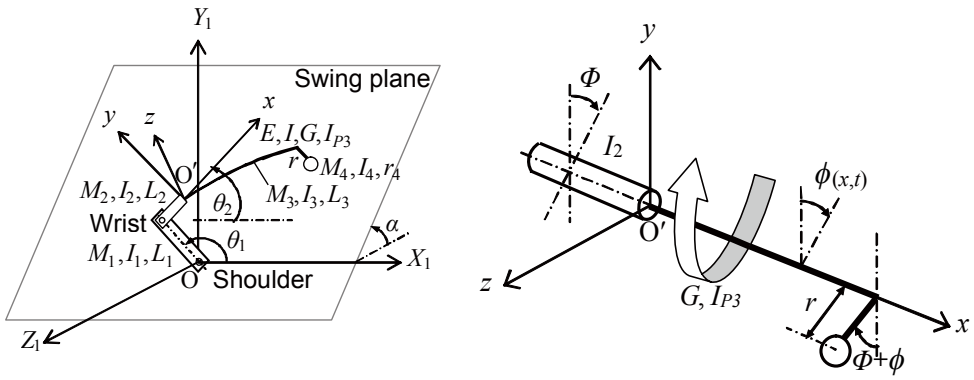

(a) Coordinate system (b) Supination of the grip

Fig. 1 Three-dimensional dynamic model

composed of two coplanar rigid segments, which represent the left arm and the hand-grip part of the golfer, can be employed. The tilt angle α of the swing plane is set at 0 or $\pi/2$ radians in the basic skill analysis, and $\pi/3$ radians for driver shots. The grip part also rotates around the longitudinal axis of the club shaft to accommodate the supination of the forearm. In the shaft vibration analysis, the shaft is assumed to be a Bernoulli-Euler beam, and the in-plane and out-of-plane bending vibrations and torsional vibration are examined by a uniform continuous cantilever beam model. The relationship between the supination angle Φ of the forearm (i.e., rotational angle of the grip part around the longitudinal axis of the club shaft) and the twist angle ϕ of the shaft is shown in Fig. 1(b). A spherical clubhead is fixed to the tip of the shaft with eccentricity r. Details of the symbols for the components of the dynamic model are provided in Appendix 1.

2.2 Equation of motion

Applying Hamilton's principle to the dynamic model, equations of motion (1) ~ (6) are derived. Equations (1) ~ (3) are equilibrium equations of moment about the shoulder, wrist, and supination, respectively. Equations (4) ~ (6) express in-plane, out-of-plane and torsional vibrations of the shaft, respectively.

$$C_1\ddot{\theta}_1+\left(C_2L_C+D_1L_S\right)\ddot{\theta}_2+\left(C_2L_S-D_1L_C\right)\dot{\theta}_2^2+2\dot{D}_1L_S\dot{\theta}_2+\ddot{D}_1L_C+G_1L_C-Q_1=0\,, \tag{1}$$

$$\begin{aligned}&\left(C_2L_C+D_1L_S\right)\ddot{\theta}_1+\left(C_3+D_2\right)\ddot{\theta}_2-\left(C_2L_S-D_1L_C\right)\dot{\theta}_1^2\\&\qquad+\dot{D}_2\dot{\theta}_2-D_3-G_2\cos\theta_2+S_1\sin\theta_2-Q_2=0\,,\end{aligned} \tag{2}$$

$$\begin{aligned}&E_1L_C\ddot{\theta}_1+E_1\left(L_2+L_3\right)\ddot{\theta}_2-E_1L_S\dot{\theta}_1^2-F_1\dot{\theta}_2^2+E_1\ddot{y}_{L_3}-E_2\ddot{z}_{L_3}\\&+\left(M_4r^2+I_4+\frac{1}{2}\left(M_2r_2^2+M_3r_3^2\right)\right)\ddot{\Phi}+\rho_3I_{P3}\int_0^{L_3}\ddot{\phi}dx+\left(I_4+M_4r^2\right)\ddot{\phi}_{L_3}-H_1-Q_3=0\,,\end{aligned} \tag{3}$$

$$\rho_3A_3\left\{\ddot{y}+L_C\ddot{\theta}_1+\left(L_2+r\right)\ddot{\theta}_2-L_S\dot{\theta}_1^2-y\dot{\theta}_2^2+g\cos\theta_2\sin\alpha\right\}+EIy''''=0, \tag{4}$$

$$\rho_3A_3\left(\ddot{z}+g\cos\alpha\right)+EIz''''=0\,, \tag{5}$$

$$\rho_3I_{P3}\left(\ddot{\Phi}+\ddot{\phi}\right)-GI_{P3}\phi''=0\,. \tag{6}$$

In these equations, the suffix "L_3" represents the deformation of the shaft at the tip; Q_1 and Q_2 are external torques applied to the shoulder and wrist joints, and Q_3 is the external torque applied around the x axis. Details of the individual terms in the equations are described in Appendix 2. Boundary conditions for the in-plane, out-of-plane, and torsion vibrations of the shaft at the tip are derived as follows:

$$\begin{aligned}&M_4L_C\ddot{\theta}_1+M_4\left(L_2+L_3\right)\ddot{\theta}_2-M_4L_S\dot{\theta}_1^2-\left(M_4y_{L_3}+E_2\right)\dot{\theta}_2^2-E_1\left(\ddot{\Phi}+\ddot{\phi}_{L_3}\right)\\&\qquad-E_2\left(\dot{\Phi}+\dot{\phi}_{L_3}\right)^2+M_4\ddot{y}_{L_3}+M_4g\cos\theta_2\sin\alpha-EIy'''_{L_3}=0\,,\end{aligned} \tag{7}$$

$$EIy''_{L_3}=0\,, \tag{8}$$

$$E_2\left(\ddot{\Phi}+\ddot{\phi}_{L_3}\right)-E_1\left(\dot{\Phi}+\dot{\phi}_{L_3}\right)^2+M_4\ddot{z}_{L_3}+M_4g\cos\alpha-EIz'''_{L_3}=0\,, \tag{9}$$

$$EIz''_{L_3}=0\,, \tag{10}$$

$$\begin{aligned}&E_1L_C\ddot{\theta}_1+E_1\left(L_2+L_3\right)\ddot{\theta}_2-E_1L_S\dot{\theta}_1^2-F_1\dot{\theta}_2^2+E_1\ddot{y}_{L_3}-E_2\ddot{z}_{L_3}\\&\qquad-\left(I_4+M_4r^2\right)\left(\ddot{\Phi}+\ddot{\phi}_{L_3}\right)-GI_{P3}\phi'_{L_3}+H_1=0\,.\end{aligned} \tag{11}$$

Then, the eigenfunction and natural angular frequency are determined by using a cantilever beam model with a spherical mass at the tip. Here, the boundary conditions for the in-plane vibration of the cantilever beam are

$$y(0,t)=y'(0,t)=0 \tag{12}$$

and

$$M_4\ddot{y}_{L_3}=EIy'''_{L_3},\quad EIy''_{L_3}=0\,. \tag{13}$$

Applying the separation of variables as in Eq.(14), the frequency equation about the in-plane vibration of the shaft is obtained as Eq. (15).

$$y(x,t)=\varphi(x)\left(A\sin\omega t+B\cos\omega t\right), \tag{14}$$

$$\frac{M_4\lambda}{M_3}\left(\cos\lambda\sinh\lambda-\sin\lambda\cosh\lambda\right)+\cos\lambda\cosh\lambda+1=0\,. \tag{15}$$

Here, λ is a nondimensional parameter of the angular frequency defined as

$$\lambda = kL_3 \quad , \quad k^4 = \frac{\rho_3 A_3}{EI}\omega^2 . \tag{16}$$

The numerical solutions to Eq. (15) are obtained by bisection, and then the natural angular frequency ω_i can be calculated. Here, the suffix "i" represents the degree of vibration mode of the shaft. Applying the orthogonal condition between the vibration modes, the eigenfunction is obtained as

$$\varphi_i(x) = \sqrt{\frac{\rho_3 A_3 L_3}{\zeta_i}}\left\{\left(\cos k_i x - \cosh k_i x\right) - f_i\left(\sin k_i x - \sinh k_i x\right)\right\}, \tag{17}$$

where

$$f_i = \frac{C'_{12}}{C'_{11}},\ \zeta_i = \frac{\rho_3 A_3 L_3}{\lambda_i}\zeta_{1i} + M_4\zeta_{2i},$$

$$C'_{11} = M_4\frac{\lambda_i}{L_3}\left(\sin\lambda_i - \sinh\lambda_i\right) - \rho_3 A_3\left(\cos\lambda_i + \cosh\lambda_i\right),$$

$$C'_{12} = M_4\frac{\lambda_i}{L_3}\left(\cos\lambda_i - \cosh\lambda_i\right) + \rho_3 A_3\left(\sin\lambda_i + \sinh\lambda_i\right),$$

$$\zeta_{1i} = \frac{1}{4}\left\{\left(1 - f_i^2\right)\sin 2\lambda_i + \left(1 + f_i^2\right)\sinh 2\lambda_i\right\} - \left(1 - f_i^2\right)\cos\lambda_i \sinh\lambda_i$$

$$- \left(1 + f_i^2\right)\sin\lambda_i \cosh\lambda_i + \frac{1}{2}f_i\left\{\cos 2\lambda_i - \cosh 2\lambda_i\right\} + 2f_i \sin\lambda_i \sinh\lambda_i + \lambda_i,$$

$$\zeta_{2i} = f_i^2\left(\sin\lambda_i - \sinh\lambda_i\right)^2 + \left(\cos\lambda_i - \cosh\lambda_i\right)^2 - 2f_i\left(\cos\lambda_i - \cosh\lambda_i\right)\left(\sin\lambda_i - \sinh\lambda_i\right).$$

The modal analysis of the out-of-plane vibration and the torsional vibration are explained in Appendix 3.

2.3 State equation

To simulate a golf swing numerically, the equations of motion must be transformed into state equations. Thus, the shaft deformation about the in-plane, out-of-plane, and torsional vibrations must be separated into displacement and time functions as follows:

$$y(x,t) = \sum_i \varphi_i(x)q_{1i}(t),\quad z(x,t) = \sum_i \eta_i(x)q_{2i}(t),\quad \phi(x,t) = \sum_i \xi_i(x)q_{3i}(t). \tag{18}$$

Where $\eta_i(x)$ and $\xi_i(x)$ are described as Eq.(A3.1) and (A3.2) in Appendix 3, respectively. By substituting Eq. (18) into Eqs.(1)~(11) and applying the orthogonal conditions between the vibration modes for bending and torsional vibrations, the equation of motion is transformed into

$$\boldsymbol{J}(\boldsymbol{v})\ddot{\boldsymbol{v}}(t) + \boldsymbol{h}(\boldsymbol{v},\dot{\boldsymbol{v}}) + \boldsymbol{g}(\boldsymbol{v},\dot{\boldsymbol{v}}) = \boldsymbol{u}(t), \tag{19}$$

where $\boldsymbol{v}$ is the generalized coordinate vector, $\boldsymbol{h}$ is the nonlinear force vector, $\boldsymbol{g}$ is the gravity term vector and $\boldsymbol{u}$ is the input vector. Only the first mode of the shaft vibration is considered to simplify the state equation. Since $\boldsymbol{J}$ is a regular matrix, Equation (19) is transformed into

$$\ddot{\boldsymbol{v}}(t) = \boldsymbol{J}^{-1}(\boldsymbol{v})\left(-\boldsymbol{h}(\boldsymbol{v},\dot{\boldsymbol{v}}) - \boldsymbol{g}(\boldsymbol{v},\dot{\boldsymbol{v}}) + \boldsymbol{u}(t)\right). \tag{20}$$

where the state variables are defined as

$$\boldsymbol{s}(\boldsymbol{t}) = \left[\boldsymbol{v}(t)^T, \dot{\boldsymbol{v}}(t)^T\right]^T = \left[\theta_1,\theta_2,\Phi,q_{11},q_{21},q_{31},\dot{\theta}_1,\dot{\theta}_2,\dot{\Phi},\dot{q}_{11},\dot{q}_{21},\dot{q}_{31}\right]^T. \tag{21}$$

Finally, the state equation of the dynamic model can be obtained as follows:

$$\dot{\boldsymbol{s}}(t) = \begin{bmatrix} \dot{\boldsymbol{v}}(t) \\ \boldsymbol{J}^{-1}(\boldsymbol{v})\left(-\boldsymbol{h}(\boldsymbol{v},\dot{\boldsymbol{v}}) - \boldsymbol{g}(\boldsymbol{v},\dot{\boldsymbol{v}}) + \boldsymbol{u}(t)\right) \end{bmatrix} = \boldsymbol{f}(\boldsymbol{s},\boldsymbol{u}). \tag{22}$$

The numerical solution of the swing motion is calculated by using the fourth-order Runge-Kutta method with time steps of 1.0×10^{-4} seconds.

3. Basic Skill Analysis

In the kinetic analysis of the golf swing, the force and torque generated by a golfer are generally investigated by inverse dynamics using an experimentally measured swing motion

Table 1 Details of the dynamic model

	Arm	Grip	Shaft	Head
L_1, L_2, L_3, r_4 (m)	0.4	0.2	1.0	2.2×10^{-2}
M_1, M_2, M_3, M_4 (kg)	3.0	1.5	2.2×10^{-1}	2.0×10^{-1}
I_1, I_2, I_3, I_4 (kg·m^2)	1.6×10^{-1}	0.1	7.4×10^{-2}	3.9×10^{-5}

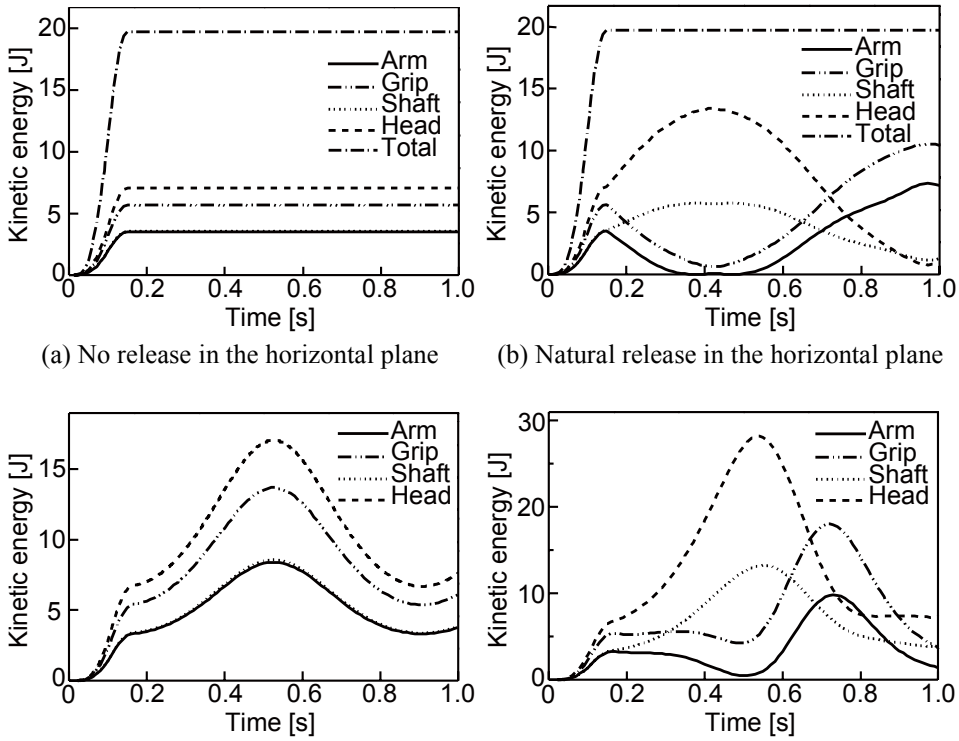

(a) No release in the horizontal plane (b) Natural release in the horizontal plane

(c) No release in the perpendicular plane (d) Natural release in the perpendicular plane

Fig. 2 Effectiveness of natural release with a rigid shaft

and a simplified dynamic model. However, the simplified model cannot effectively account for the intricate skills of an expert golfer in the inverse dynamics analysis. Thus a swing motion that can efficiently achieve a fast head speed was assumed, and this motion is examined by forward dynamics in this analysis. It is generally known that there are differences between the swing motions of expert and beginner golfers in the wrist release. Therefore, this skill is analyzed by considering the wrist release of expert golfers, such as "natural release" and "late hitting." To simplify this basic discussion, the shaft is treated as either a rigid or a flexible beam, and the inclination angle of the swing plane α is set at 0 or π/2 radians (i.e., the swing plane is horizontal or perpendicular) in the two-dimensional model without supination of the grip or out-of-plane and torsional vibrations of the shaft. Specifications of the model are shown in Table 1.

3.1 Natural release

An efficient swing with a fast head speed is examined on the assumption that "natural release" is a completely passive wrist movement without active torque involved in the wrist release in the swing plane. Initially, θ_1 and the relative angle between the center axes of the arm and the grip (i.e., π-θ_1+θ_2) are set to π/2 radians. At the start of the swing, the shoulder is accelerated by the torque of the shoulder joint and the wrist is fixed to maintain the initial angle only by the geometric constraint (i.e., the wrist is assumed to be a hinge joint with a stopper). Then the wrist is naturally released by the change in the constraint condition between the joints and by the balance of the force and moment of the swing model

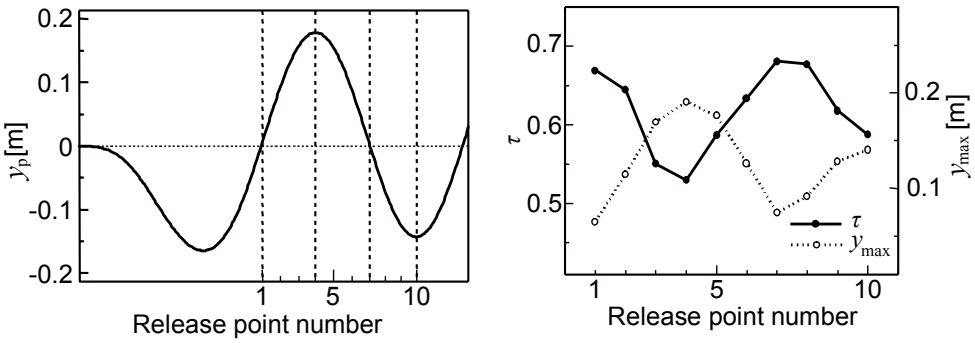

(a) Release points based on shaft deformation

(b) Variation in efficiency index and maximum shaft deformation

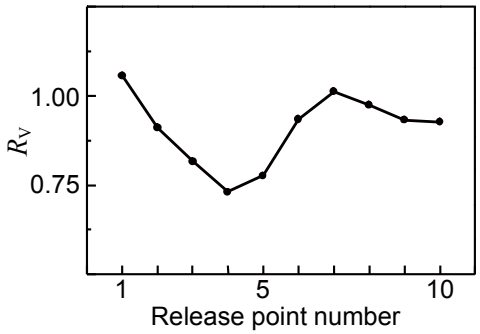

(c) Variation in the rate of head speed at impact

Fig. 3 Effectiveness of natural release with a flexible shaft

according to the attitude and angular velocities of the joints. After the release, the rotation of the grip completely depends on the moment around the wrist joint. Thus, in the latter half of the swing motion, both the shoulder and wrist joints become free. In the final state of the swing, the center axes of the arm and grip should be straight without adjusting the attitude of the model by the joint torque. Figures 2(a) and (b) show the variations in kinetic energy for each part in the horizontal swing plane with the rigid shaft, and Figs. 2(c) and (d) show the variations in kinetic energy in the perpendicular swing plane. In both cases, the wrist is naturally released immediately after the acceleration of the shoulder is complete, and the variation pattern of the kinetic energy can be categorized into shaft-head and arm-grip groups. The kinetic energy of the shaft-head group is maximized when the energy of the arm-grip group is minimized. The kinetic energy of the head under "natural release" is increased by 90% in Fig. 2(b) and 62% in (d) compared to the energy of the case with no release. This indicates that a "natural release" can effectively increase the head speed without active motion of the wrist by utilizing the interference force, which naturally stops the arm movement. When the shaft is assumed to be flexible, the wrist is naturally released at the zero-crossing point of the bending deformation of the shaft vibration, in which a large change occurs on the balance of the force and moment. Expert golfers place special emphasis on selecting a club shaft where the flexibility complements their swing style. Therefore, it is expected that the "natural release" is closely related to the bending vibration during the swing. Here, as shown in Fig. 3(a), we specify ten release points that coincide with deformation of the shaft vibration. In this figure, y_p represents the displacement at the tip of the shaft while the wrist is fixed in the down swing. The time from the first zero-crossing point of y_p to the minimum point of displacement is equally divided into ten release points.

The bending rigidity EI is set at 80 [N·m^2]. Except at the zero-crossing point, the wrist of the gofer is constrained to resist the "natural release" to adjust to other release points. Therefore, the wrist release for each case, except for the zero-crossing point, needs some exertion from the wrist. The efficiency index τ, which is used to evaluate the proficiency degree of these swing motions, is calculated as the ratio of kinetic energy E_h of the club

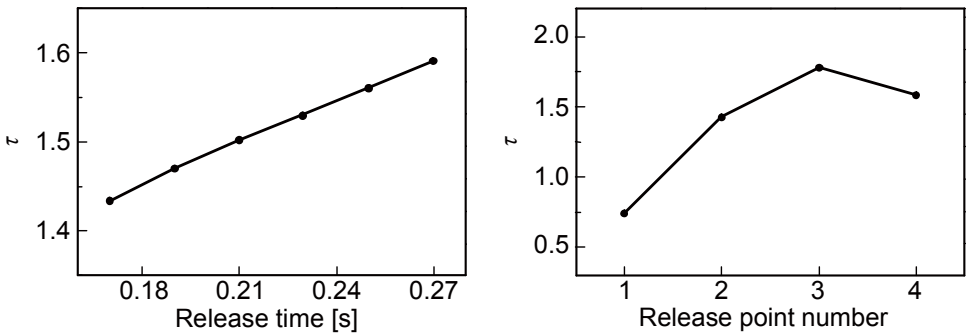

(a) Efficiency index with a rigid shaft (b) Efficiency index with a flexible shaft

Fig. 4 Effectiveness of late hitting

head at the impact to the work done by the torque $Q_1(t)$ of the shoulder as follows:

$$\tau = \frac{E_h}{\int_{\theta_1} Q_1(t) d\theta_1}. \tag{23}$$

Figure 3(b) shows τ and the maximum displacement y_{max} of the shaft at the final zone for each release point under the same work done by the torque of the shoulder. The final zone is determined as a range within ± 0.02 seconds of the impact. It is demonstrated that τ becomes larger with the "natural release" at the zero-crossing point, and that the maximum displacement simultaneously decreases. This indicates that much of the shaft's elastic strain energy is transformed into the kinetic energy of the club head by the zero-crossing release. Under the same conditions of the swing motion, the ratio of head speed between flexible and rigid shafts R_V is shown in Fig. 3(c). The release at the first zero-crossing achieves a maximum head speed, and the release at the maximum displacement achieves approximately a 26% reduction of the head speed from the speed with a rigid shaft. As a result, it is suggested that "natural release" is a skill helping to achieve a fast head speed utilizing interference between the wrist and shoulder joints and shaft elasticity.

3.2 Late hitting

The primary difference between the swing motions of expert and beginner golfers lies in the timing of the wrist release. The expert golfer is capable of maintaining the initial wrist angle longer than the beginner during the downswing. When the wrist movement termed "late hitting" is examined by using the energy balance, the potential energy may be expected to strongly affect the movement of each part of the body of the golfer. Thus, in a perpendicular swing plane, the relationship between the release timing and τ was examined, as shown in Fig. 4. In the case of the rigid shaft (Fig. 4(a)), it is demonstrated that the value of τ increases in proportion to the release time. When the wrist is released early, the arm and grip are accelerated by using much of the potential energy. Therefore, the kinetic energy of the club head is reduced. In the flexible shaft case, τ is maximized at release point number 3, as shown in Fig. 4(b). This indicates that the potential energy affects the head speed more strongly than the strain energy of the shaft. With a long club like the driver, the effect of the potential energy is not so pronounced because the angle of inclination of the swing plane is smaller than that with shorter clubs. Therefore, it is advantageous to delay the zero-crossing point, to utilize both the potential and kinetic energies for a fast head speed with the natural and late release in the actual swing motion.

4. Three-dimensional Skill Analysis

The three-dimensional golf swing motion used for this analysis is simply illustrated in Fig. 5. The motion is very similar to the two-dimensional model except for the supination of the grip and the addition of α. The supination torque is input between the release point of the wrist and the impact with the ball, the angle α is set at $\pi/3$ rad for a driver shot, and so

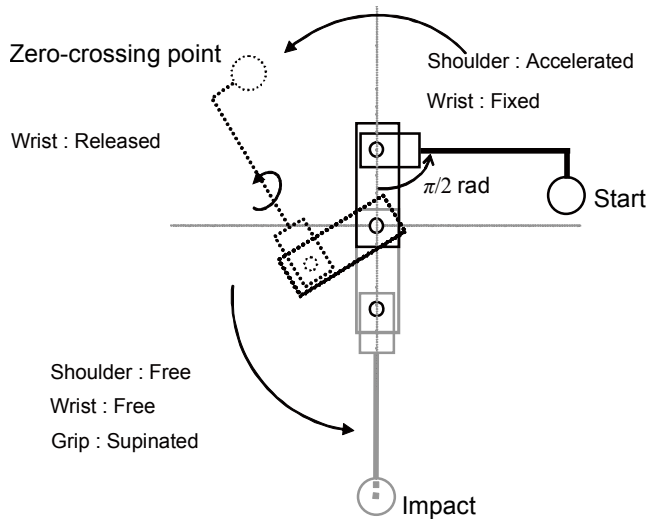

Fig. 5 Basic settings of the golf swing motion

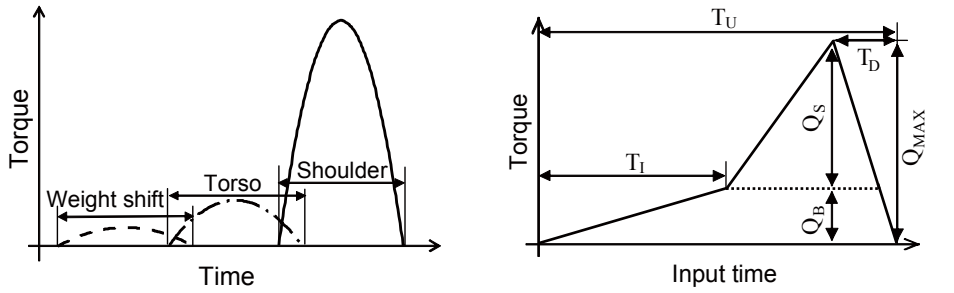

(a) Composite acceleration torque of the whole body motion

(b) Simplified two-step modulation torque

Fig. 6 Input torque of the shoulder joint

three-dimensional bending and torsional vibrations occur on the club shaft.

4.1 Wrist release

The basic skill analysis demonstrated that delaying the zero-crossing point of the shaft vibration was the most important for efficiently achieving a fast head speed. To delay the zero-crossing point, the torque input of the shoulder joint has to increase during the acceleration of the arm in the simplified model. However, it is extremely difficult to accelerate the downswing by only the movement of the shoulder. Thus, it may be expected that expert golfers delay the zero-crossing point by utilizing their whole body motion. Consequently, it can be assumed that the acceleration torque is generated by the weight shifting and torso twist and shoulder rotation, as shown in Fig. 6(a). Then, the acceleration torque is simplified to a two step modulation torque, as shown in Fig. 6(b). Here, Q_{MAX}, which is the sum of Q_B and Q_S, represents the maximum possible acceleration torque that is determined by the golfer's physical strength. A feature of the whole body motion will be simulated by the total input time T_U, the first increase time T_I and the last decrease time T_D. The validity of this torque function in delaying the zero-crossing point can be examined by comparing simple trapezoidal and triangular functions that were examined in a previous study by Suzuki et al.[12]. Figure 7(a) shows the relationship between the shoulder joint angle at the wrist release θ_r and Q_{MAX} for three types of functions with the same work input by the shoulder. Similarly, the relationship between τ and the head speed at impact V_h is shown in Fig. 7(b). Here θ_r also shows the position of the arm at the zero-crossing point, because the wrist is always released at the zero-crossing point by "natural release." As a result, it was clarified that an increase in the acceleration torque with the whole body motion can delay the zero-crossing point and efficiently achieve a fast head speed. In other

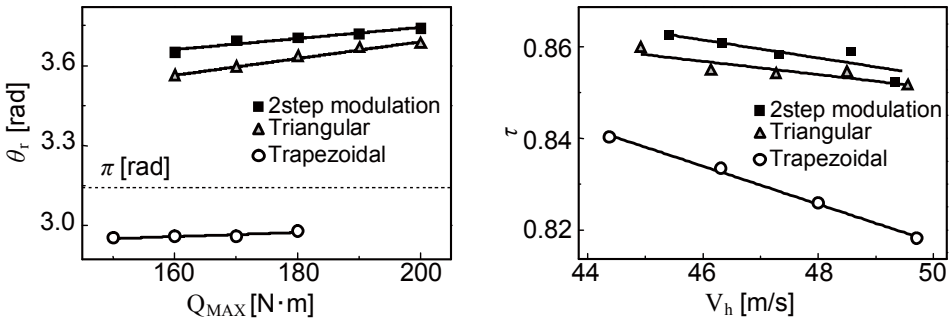

(a) Shoulder joint angles at the wrist release (b) Efficiency indices

Fig. 7 Importance of whole body motion for an effective wrist release

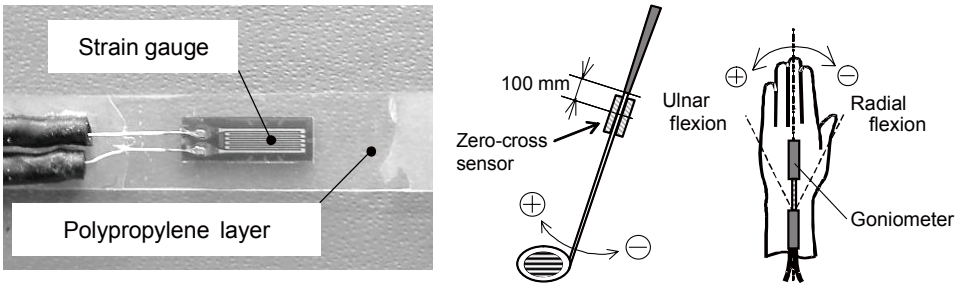

(a) Zero-crossing sensor (b) Measurement of zero-crossing point and wrist release point

Fig. 8 Experimental equipment

words, expert golfers achieve "natural release" and "late hitting" by a harmonization between the whole body motion and the dynamics of the flexible shaft, to efficiently achieve a faster head speed.

5. Experimental Verification

5.1 Experimental Method

To demonstrate the validity of the skill analysis, it was experimentally investigated whether expert golfers achieve "late hitting" by delaying the zero-crossing point. As shown in Fig. 8(a) and (b), the shaft deformation was measured by a "Zero-cross sensor" that is composed of a strain gauge and an attachable polypropylene layer. The release point is defined by a change in the radial-ulnar angle of the left wrist measured by a goniometer. In the experiments, seven subjects with various official handicaps swung their own driver. The swing motion was captured by a Vicon Motion Systems (VICON, OMG) set up.

5.2 Skill Evaluation

Figure 9(a) shows the time till the release point of the wrist, the zero-crossing point, and the impact, represented by Tr, Tz, and Ti, respectively. The subjects swung their own golf clubs and hit a light plastic imitation ball three times. The ratio of the release time to the zero-crossing time Tr/Tz, the ratio of Tz to the downswing time Tz/Ti and the ratio of Tr to the downswing time Tr/Ti shown in Fig. 9 (b). It demonstrates that the zero-crossing point was later and the release point was closer to the zero-crossing point in the downswing as the skill level of the golfer increased. However, all subjects naturally released the wrist at the zero-crossing point. This suggests that the shaft vibration strongly affects the movement of the wrist joint. As a result, the analytical results of the influence of skill on the wrist release were experimentally verified. Figure 10 shows the results of the swing motion analysis measured by VICON to examine the optimum induced skill timing of weight shift, torso twist, and shoulder rotation. The timing that is calculated by the second order

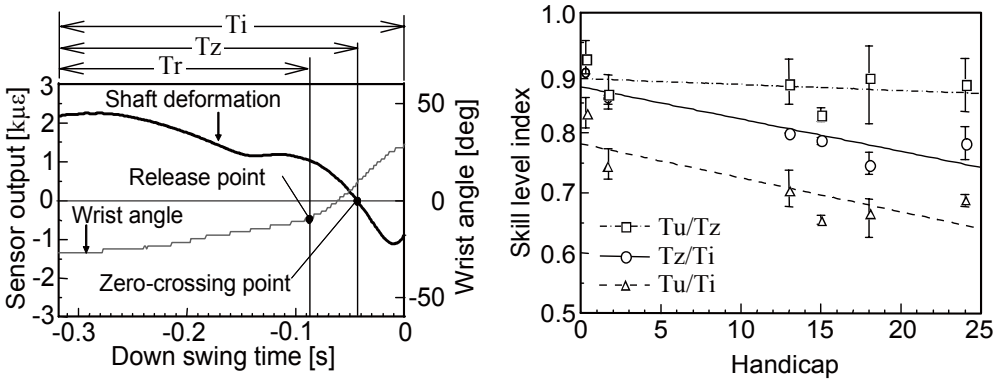

(a) Skill level parameters (b) Skill level index differences

Fig. 9 Experimental results of skill evaluation

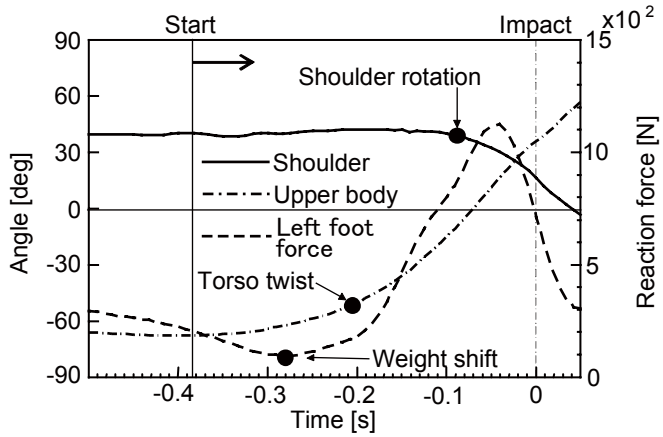

Fig. 10 Whole-body swing motion of an expert golfer (Hcp =0.3)

difference is marked with black dots in the figure. It is also demonstrated that an expert golfer can gradually change the movement of the body from the lower part to the upper part during the downswing. This suggests that the expert golfer can accelerate the rotation of the shoulder in the latter half of the downswing, and can delay the zero-crossing point.

6. Conclusions

The skill employed by expert golfers including "natural release" and "late hitting" were examined using a simplified dynamic model and the analysis was substantiated by experiments. As a result, it was analytically demonstrated that "natural release" at the zero-crossing point of the bending vibration of the shaft could efficiently increase the head speed at impact. Next, the "late hitting" condition was imposed upon the model by assuming the effect of the whole body motion in the shoulder torque input. The experimental results indicated that "late hitting" at the zero-crossing point could be carried out by increasing the shoulder acceleration torque, and could further improve the efficiency of the swing motion by utilizing the potential energy. Finally, the skill component of the swing of expert golfers was experimentally supported by measurements of the movement of the wrist and the dynamic deformation of the shaft during the downswing.

References

(1) Cochlan, A. J. and Stobbs, J., *Search for the perfect swing*, (1968), Triumph Books London: Morrison & Gibb Ltd.

(2) Lampsa, M. A., Maximizing Distance of the Golf Drive: An Optimal Control Study, *Transactions of the ASME, Journal of Dynamic Systems, Measurement, and control*, Vol.75

(1975), pp.362-367.
(3) Budney, D.R. and Bellow, D. G., On the Swing Mechanics of a Matched Set of Golf Clubs, *Research Quarterly for Exercise and Sport*, Vol.53 (1982), pp.185-192.
(4) Butler, J.H. and Winfield, D.C. The Dynamic Performance of the Golf Shaft during the Downswing, *In: Science and Golf II: Proceedings of the World Scientific Congress of Golf (eds A.J. Cochran & M.R. Farrally)*, E & FN Spon, London, UK, (1994), pp. 259-264.
(5) Brylawski, A.M., An Investigation of Three Dimensional Deformation of a Golf Club during Downswing, *In: Science and Golf II: Proceedings of the World Scientific Congress of Golf (eds A.J. Cochran & M.R. Farrally)*, E & FN Spon, London, UK, (1994), pp. 265-270.
(6) Milne, R. D. and Davis, J. P., The Role of the Shaft in the Golf Swing, *Journal of Biomechanics*, Vol.25 (1992), pp.975-983.
(7) Jorgensen, T., On the Dynamics of the Swing of a Golf Club, *American Journal of Physics*, Vol.38 (1970), pp.644-651.
(8) Vaughan, C. L., A Three-Dimensional Analysis of the Forces and Torques Applied by a Golfer during the Down Swing, *Biomechanics VII-B (edited by Morecki et al.)*, Polish Scientific Publishers, Warsaw, (1981), pp. 325-331.
(9) Neal, R.J. and Wilson, B.D., 3D Kinematics and Kinetics of the Golf Swing, *International Journal of Sports Biomechanics*, Vol.1 (1985), pp.221-232.
(10) Pickering, W.M. and Vickers, G.T., On the Double Pendulum Model of the Golf Swing, *Journal of Sports Engineering*, Vol.2 (1999), pp.161-172.
(11) Springs, E.J. and Mackenzie, S.J., Examining the Delayed Release in the Golf Swing Using Computer Simulation, *Journal of Sports Engineering*, Vol.5 (2002), pp.23-32.
(12) Suzuki, S., Hoshino, Y., Kobayashi, Y. and Kazahaya, M., Skill Analysis of the Wrist Turn in a Golf Swing to Utilize Shaft Elasticity, *The Impact of Technology on sports II* (2007), pp.259-264.

Appendix 1

List of components

Suffixes (*) 1:Arm, 2:Grip part, 3:Shaft, 4:Head

M_* [kg]: Mass

I_* [kg·m^2]: Moment of inertia around the center of gravity

L_* [m]: Length

r_* [m]: Radius of cross section

r [m]: Offset of a club head

E [N/m^2]: Young's modulus of a shaft

G [N/m^2]: Sheer modulus of a shaft

I [m^4]: Moment of inertia of cross section of a shaft

I_P [m^4]: Polar moment of inertia of cross section of a shaft

θ_1 [rad]: Rotational angle of a shoulder joint

θ_2 [rad]: Rotational angle of a wrist joint

α [rad]: Inclination angle of a swing plane

Appendix 2

Details of terms in the equations

$$L_S = L_1 \sin(\theta_1 - \theta_2),\ L_C = L_1 \cos(\theta_1 - \theta_2),$$

$$C_1 = I_1 + (M_2 + M_3 + M_4)L_1^2,\ C_2 = \frac{1}{2}M_2 L_2 + M_3\left(L_2 + \frac{1}{2}L_3\right) + M_4(L_2 + L_3),$$

$$C_3 = I_2 + I_3 + I_4 + M_3 L_2(L_2 + L_3) + M_4(L_2 + L_3)^2,$$

$$D_1 = \rho_3 A_3 \int_0^{L_3} Y dx + M_4 Y_{L_3} + M_4 r \cos(\phi_1 + \phi_{L_3}),$$

$$D_2 = \rho_3 A_3 \int_0^{L_3} Y^2 dx + M_4 Y_{L_3}^2 + M_4 r^2 \cos^2(\phi_1 + \phi_{L_3}) + 2M_4 r Y_{L_3} \cos(\phi_1 + \phi_{L_3}),$$

$$D_3 = \rho_3 A_3 \int_0^{L_3} (L_2 + r)\ddot{Y} dx + M_4 (L_2 + L_3)\ddot{Y}_{L_3}$$
$$- M_4 (L_2 + L_3) r(\ddot{\phi}_1 + \ddot{\phi}_{L_3}) \sin(\phi_1 + \phi_{L_3}) - M_4 (L_2 + L_3) r(\ddot{\phi}_1 + \ddot{\phi}_{L_3})^2 \cos(\phi_1 + \phi_{L_3})$$

$$E_1 = M_4 r \sin(\phi_1 + \phi_{l_3}), \quad E_2 = M_4 r \cos(\phi_1 + \phi_{l_3}),$$

$$F_1 = M_4 r \cos(\phi_1 + \phi_{l_3}) \sin(\phi_1 + \phi_{l_3}) + M_4 r Y_{L_3} \sin(\phi_1 + \phi_{l_3}),$$

$$G_1 = \left(\frac{1}{2} M_1 + M_2 + M_3 + M_4 \right) g \sin\phi,$$

$$G_2 = \left\{ \frac{1}{2} M_2 L_2 + M_3 \left(L_2 + \frac{1}{2} L_3\right) + M_4 (L_2 + L_3) \right\} g \sin\alpha,$$

$$H_1 = M_4 g r \cos\theta_2 \sin(\phi_1 + \phi_{l_3}) \sin\alpha - M_4 g r \cos(\phi_1 + \phi_{l_3}) \cos\alpha,$$

$$S_1 = \left\{ \rho_3 A_3 \int_0^{L_3} Y dx + M_4 r \cos(\phi_1 + \phi_{l_3}) + M_4 Y_{L_3} \right\} g \sin\alpha.$$

Appendix 3

Modal analysis of the out-of-plane vibration and torsional vibration of the club shaft are described here.

First, the modal analysis of the out-of-plane vibration is explained. Like the analysis of the vibration mode about the in-plane vibration, the boundary conditions of the out-of-plane vibrations are

$z(0,t) = z'(0,t) = 0$, and $M_4 \ddot{z}_{L_3} = EIz'''_{L_3}$, $EIz''_{L_3} = 0$.

Applying the separation of variables as

$z(x,t) = \eta(x) e^{j\omega t}$.

the frequency equation about the out-of-plane vibration of the shaft is obtained by the same expression as Eq.(15). Therefore, the angular frequencies, ω_i, and the vibration modes are obtained in the same way as the in-plane vibration, and the vibration mode has the same expression as Eq.(17) as

$$\eta_i(x) = \sqrt{\frac{\rho_3 A_3 L_3}{\zeta_i}} \left\{ (\cos k_i x - \cosh k_i x) - f_i (\sin k_i x - \sinh k_i x) \right\}. \tag{A3.1}$$

Next, the modal analysis of the torsional vibration is explained. The boundary conditions of the torsional vibration are

$\phi(0,t) = 0$, and $\left(I_4 + M_4 r^2\right)\ddot{\phi}_{L_3} + GI_{P3}\phi'_{L_3} = 0$.

Applying the separation of variables as

$\phi(x,t) = \xi(x) e^{j\Omega t}$,

the frequency equation about the torsional vibration of the shaft is obtained as

$$\left(\frac{G\lambda_\xi}{\rho_3 L_3}\right)^2 (M_4 r^2 + I_4) \sin\lambda_\xi + GI_P \left(\frac{\lambda_\xi}{L_3}\right) \cos\lambda_\xi = 0$$

where

$$\Omega = \frac{G}{\rho_3 L_3} \lambda_\xi.$$

The natural angular frequencies Ω_i are calculated in the same way as the bending vibrations by using the bisection method. Here, the suffix "i" represents the degree of vibration mode of the shaft. The eigenfunction about the torsional vibration is obtained as

$$\xi_i(x) = \sqrt{\frac{\rho_3 I_P L_3}{\sigma_i}} \sin k_{\xi i} x \tag{A3.2}$$

where

$$\sigma_i = \frac{\rho_3 I_P L_3}{\lambda_{\xi i}} \left(\frac{\lambda_{\xi i}}{2} - \frac{\sin 2\lambda_{\xi i}}{4} \right) + (M_4 r^2 + I_4) \sin^2 \lambda_{\xi i}, \quad \lambda_{\xi i} = k_{\xi i} L_3.$$